The complete non-spinning effective-one-body metric at linear order in the mass ratio

Enrico Barausse,[1] Alessandra Buonanno,[1,2] and Alexandre Le Tiec[1]

[1] *Maryland Center for Fundamental Physics & Joint Space-Science Institute, Department of Physics, University of Maryland, College Park, MD 20742*

[2] *Radcliffe Institute for Advanced Study, Harvard University, 8 Garden St., Cambridge, MA 02138*

(Dated: May 22, 2014)

Using the main result of a companion paper, in which the binding energy of a circular-orbit non-spinning compact binary system is computed at leading-order beyond the test-particle approximation, the exact expression of the effective-one-body (EOB) metric component $g_{tt}^{\rm eff}$ is obtained through first order in the mass ratio. Combining these results with the recent gravitational self-force calculation of the periastron advance for circular orbits in the Schwarzschild geometry, the EOB metric component $g_{rr}^{\rm eff}$ is also determined at linear order in the mass ratio. These results assume that the mapping between the real and effective Hamiltonians at the second and third post-Newtonian (PN) orders holds at all PN orders. Our findings also confirm the advantage of resumming the PN dynamics around the test-particle limit if the goal is to obtain a flexible model that can smoothly connect the test-mass and equal-mass limits.

PACS numbers: 04.25.D-, 04.25.dg, 04.25.Nx, 04.30.-w

I. INTRODUCTION

Although the "two-body problem" cannot be solved analytically in the general theory of relativity, at least two approximation methods can be used to tackle it. The first one dates back to Einstein's 1915 calculation of the relativistic perihelion advance of Mercury's orbit [1], and is based on a perturbative treatment in powers of the ratio v/c between the binary's relative velocity v (in the center-of-mass frame) and the vacuum speed of light c. At the lowest order of approximation, this approach gives back the well-known Newtonian solution, and is therefore dubbed "post-Newtonian" (PN) expansion; see *e.g.* Ref. [2] and references therein. Currently, the two-body dynamics of non-spinning compact objects is known through 3PN order[1] [3, 4], and the gravitational-wave fluxes of energy and angular momentum through 3.5PN [5–7] and 3PN [8] orders for circular and eccentric orbits, respectively. Spin effects have also been computed in the dynamics and gravitational radiation [9–11] using both Hamiltonian [12–16] and Lagrangian [9, 17] formulations. The effective-field-theory approach applied to gravity [18] has confirmed some of these results [19, 20], and has pushed the calculations to higher PN orders for spinning bodies [20–27].

The second approximation method also dates back to 1915, namely to Karl Schwarzschild's famous wartime calculation of the gravitational field of a spherically symmetric body [28, 29]. While non-rotating black holes are described by the Schwarzschild metric, rotating black holes are represented by the Kerr solution [30]. The motion of test masses in the Schwarzschild or Kerr geometries is naturally described by the geodesic equations, which are valid for arbitrarily high values of the orbital velocity v (*i.e.* the geodesic equations formally include all PN corrections). If the finite mass of the particle and its backreaction on the background geometry are taken into account, the orbits will deviate from geodesic motion under the effect of the gravitational self-force (GSF) [31]. More formally, Schwarzschild or Kerr geodesics can be seen as the orbital motion of the binary at the zeroth order of approximation in the mass ratio, while at first order the two-body dynamics is regulated by the so-called "MiSaTaQuWa" equation [32, 33]. The GSF can be split into a dissipative component related to gravitational-wave emission — which is described by the Regge-Wheeler and Zerilli equations in a Schwarzschild background [34, 35], and by the Teukolsky equation in Kerr [36, 37] —, and a conservative component responsible for secular effects such as the periastron advance [38–40].

A notable event in the history of the general relativistic two-body problem took place almost a century after Einstein's and Schwarzschild's early work, in 2005, with the first numerical simulations of the inspiral, merger, and ringdown of a system of two non-spinning black holes [41–43]. While these results constitute a truly remarkable achievement, current "state-of-the-art" numerical relativity (NR) simulations are still too time-consuming to provide gravitational waveforms covering the whole parameter space of binary black-hole systems, especially for small mass ratios [44] and black holes with large spins [45, 46].

A semi-analytical approach that is flexible enough to incorporate information from both PN expansions and

[1] As usual we refer to nPN as the order corresponding to terms $\mathcal{O}(c^{-2n})$ with respect to the Newtonian acceleration in the equations of motion, or with respect to the quadrupole formula in the radiation field.

black-hole perturbations, as well as from NR simulations, is the effective-one-body (EOB) method [47]. The basic idea behind this construction is to map the orbital dynamics of an arbitrary mass-ratio compact binary system onto that of a test particle in a suitable background spacetime. In order for the EOB model to have the correct test-particle limit, this effective background metric, $g^{\rm eff}_{\alpha\beta}$, must clearly reduce to that of a Schwarzschild black hole when one of the masses goes to zero (for non-spinning binaries). In addition, such a mapping is known to exist for *any* mass ratio at the Newtonian level, because in Newtonian gravity one can always map the dynamics of a binary system with masses m_1 and m_2 onto the motion of an effective particle with reduced mass $\mu = m_1 m_2/(m_1+m_2)$ around a body with total mass $M = m_1 + m_2$. It is therefore natural to try to achieve the EOB mapping by considering an effective particle with mass μ moving in a time-independent and spherically symmetric *deformed* Schwarzschild spacetime with total mass M,[2]

$$ {\rm d}s^2_{\rm eff} = g^{\rm eff}_{tt}(r;\nu)\,{\rm d}t^2 + g^{\rm eff}_{rr}(r;\nu)\,{\rm d}r^2 + r^2{\rm d}\Omega^2\,, \qquad (1.1) $$

where the deformation is regulated by the symmetric mass ratio $\nu \equiv \mu/M$. In the test-particle limit $\nu \to 0$, we recover (by construction) the Schwarzschild result $g^{\rm eff}_{tt} = -1/g^{\rm eff}_{rr} = -1 + 2M/r$. Beyond that limit, the ν-dependence of the EOB potentials $g^{\rm eff}_{tt}$ and $g^{\rm eff}_{rr}$ encodes crucial information about the dynamics of the real binary system.

Buonanno and Damour [47] showed that, for spinless binaries, the EOB mapping can be achieved not only at the Newtonian level, but also at the 1PN and 2PN orders, obtaining the following relation between the Hamiltonian $H_{\rm real}$ of the real binary system and the Hamiltonian $H_{\rm eff}$ of the effective particle:

$$ H_{\rm real} = M\sqrt{1 + 2\nu\left(\frac{H_{\rm eff}}{\mu} - 1\right)}. \qquad (1.2) $$

Remarkably, this formula coincides with that introduced by Brézin, Itzykson and Zinn-Justin [48] in quantum electrodynamics to map the one-body relativistic Balmer formula with the two-body one; for example it can relate some of the energy levels of positronium (an equal-mass system comprised of an electron and an anti-electron, described by the real two-body Hamiltonian $H_{\rm real}$) to those of the hydrogen atom (an "extreme" mass-ratio system described by the effective Hamiltonian $H_{\rm eff}$).

Since the original paper [47], the EOB mapping has been extended to 3PN order for non-spinning binaries [49], and shown to exist also for spinning binaries, through 3.5PN order in the spin-orbit terms, and 2PN order in the spin-spin terms [50–55]. Furthermore, the EOB construction has grown to include a model for the gravitational waveforms [56–60], allowing detailed comparisons (and calibrations of the EOB model's unknown parameters) with NR waveforms for non-spinning and spinning comparable-mass binaries [61–71], as well as with Regge-Wheeler-Zerilli [57, 72–75] and Teukolsky waveforms [60, 76–78] for small and extreme mass-ratios.

More recently, information coming from GSF calculations has started to be included into the EOB model. References [53, 71, 79] used the frequency shift of the Schwarzschild innermost stable circular orbit (ISCO) induced by the conservative GSF, as recently calculated by Barack and Sago [39] (see also Ref. [80]), to constrain some unknown parameters entering the $g^{\rm eff}_{tt}$ component of the EOB effective metric (1.1) for spinless binaries, and regulating the unknown higher PN orders. Ref. [79] also suggested using GSF data to determine a certain combination $\rho_{\rm SF}$ of the free functions parametrizing the $g^{\rm eff}_{tt}$ and $g^{\rm eff}_{rr}$ components of the EOB effective metric, at linear order in the mass ratio. That suggestion was then realized in Ref. [81], which calculated the strong-field behavior of $\rho_{\rm SF}$ using the GSF contribution to the periastron advance for quasi-circular orbits in a Schwarzschild background.

Besides the ISCO frequency shift and the periastron advance, a third physically meaningful (*i.e.* coordinate invariant) perturbative result that has been obtained within the GSF framework is the conservative effect of the self-force on the "redshift observable" $z \equiv -u_\alpha K^\alpha$, u^α being the particle's four-velocity and K^α the helical Killing vector of the perturbed Schwarzschild geometry [38, 82–85]. Refs. [38, 84, 85] (see also [86]) demonstrated a very good agreement between the numerical GSF result and the PN prediction.

The quantity z measures the redshift of light rays emitted from the particle, and received far away from the binary system, along the helical symmetry axis perpendicular to the orbital plane [38]. In the companion paper [87], we put forward a different interpretation for the redshift observable. Building on the first law of binary point-particle mechanics recently established in Ref. [88], we relate z to the binding energy of a binary system of non-spinning compact objects through next-to-leading order in the mass ratio. Using the numerical results of Refs. [38, 82–85], in which the GSF contribution to the redshift observable of a non-spinning particle moving on a circular orbit around a Schwarzschild black hole was calculated, we derive an explicit expression for the binding energy.

In this paper, we use this new result for the binding energy, assuming that the mapping (1.2) holds at all PN orders, to derive the *exact* expression of the $g^{\rm eff}_{tt}$ component of the EOB effective metric (1.1) for non-spinning binaries, through *linear* order in the mass ratio. The resulting expression exactly reproduces the ISCO frequency shift calculated by Barack and Sago, and goes far beyond the results of Refs. [53, 71, 79] that could only constrain certain combinations of unknown parameters appearing in the EOB potential $g^{\rm eff}_{tt}$.

[2] Throughout this paper we use geometrical unit $G = c = 1$.

Moreover, thanks to the exact knowledge (at least through linear order in the mass ratio) of $g^{\rm eff}_{tt}$, we are able to use the GSF results of Ref. [79, 81] for the periastron advance to determine the EOB metric component $g^{\rm eff}_{rr}$ *exactly* (through linear order in the mass ratio) for non-spinning binaries. This constitutes significant advance over earlier results that could only constrain combinations of unknown functions entering $g^{\rm eff}_{tt}$ and $g^{\rm eff}_{rr}$. Our results therefore completely determine the EOB effective metric (1.1) for a system of non-spinning compact objects, at first order in the mass ratio.

This paper is organized as follows. In Sec. II, after briefly reviewing the EOB effective metric and Hamiltonian dynamics, we use the binding energy computed in Ref. [87] to derive the exact correction to $g^{\rm eff}_{tt}$ that is linear in the mass ratio. Moreover, employing the results of the periastron advance for circular orbits from Refs. [79, 81], we also derive the exact term linear in the mass ratio in $g^{\rm eff}_{rr}$. In Sec. III we use the binding energy computed through 6PN order in Ref. [88], together with several constraints among the EOB metric coefficients derived in Refs. [79, 81], to compute $g^{\rm eff}_{tt}$ and $g^{\rm eff}_{rr}$ through 6PN and 5PN orders, respectively, at linear order in the mass ratio. Finally, in Sec. IV we discuss the main results of the paper and comment on future work. The structure of the EOB Hamiltonian used in the rest of this paper is detailed in an Appendix.

II. SELF-FORCE CONTRIBUTIONS TO THE EOB POTENTIALS

Within the EOB framework, the real Hamiltonian $H_{\rm real}$ encoding the orbital dynamics of two non-spinning compact objects is mapped to an *effective* Hamiltonian $H_{\rm eff}$ describing a test particle of mass $\mu = m_1 m_2/(m_1+m_2)$ moving in a *deformed* Schwarzschild metric of mass $M = m_1 + m_2$. The deformation is regulated by the binary's symmetric mass ratio $\nu = \mu/M$, and disappears in the test-particle limit $\nu \to 0$. The EOB effective metric reads [47]

$$ {\rm d}s^2_{\rm eff} = -A(r)\,{\rm d}t^2 + B(r)\,{\rm d}r^2 + r^2 {\rm d}\Omega^2 \,, \tag{2.1} $$

where the potentials $A \equiv -g^{\rm eff}_{tt}$ and $B \equiv g^{\rm eff}_{rr}$ are known through 3PN order [47, 49]. We find it more convenient to work with the potential $\bar{D} \equiv (AB)^{-1}$, so that

$$ A(u) = 1 - 2u + 2\nu\,u^3 + \left(\frac{94}{3} - \frac{41}{32}\pi^2\right)\nu\,u^4 + \mathcal{O}(u^5) \,, \tag{2.2a} $$

$$ \bar{D}(u) = 1 + 6\nu\,u^2 + (52 - 6\nu)\,\nu\,u^3 + \mathcal{O}(u^4) \,, \tag{2.2b} $$

where $u \equiv M/r$ denotes the inverse Schwarzschild-like EOB radial coordinate. In the test-particle limit $\nu \to 0$, we recover (by construction) the Schwarzschild results $A(u) = 1 - 2u$ and $\bar{D}(u) = 1$. Through 3PN order, the effective Hamiltonian is given by [47, 49]

$$ H^2_{\rm eff}(\boldsymbol{r},\boldsymbol{p}) = \mu^2 A(r)\left[1 + \hat{\boldsymbol{p}}^2 + \left(B(r)^{-1} - 1\right)(\boldsymbol{n}\cdot\hat{\boldsymbol{p}})^2 + 2(4-3\nu)\,\nu\,u^2\,(\boldsymbol{n}\cdot\hat{\boldsymbol{p}})^4\right] , \tag{2.3} $$

where we introduced the reduced conjugate momentum $\hat{\boldsymbol{p}} = \boldsymbol{p}/\mu$ and the unit vector $\boldsymbol{n} = \boldsymbol{r}/r$. Finally, the so-called improved real (or EOB) Hamiltonian reads [47]

$$ H_{\rm EOB} \equiv H^{\rm improved}_{\rm real} = M\sqrt{1 + 2\nu\left(\frac{H_{\rm eff}}{\mu} - 1\right)} \,. \tag{2.4} $$

When extending the EOB Hamiltonian (2.4) to higher PN orders, one needs to modify the effective dynamics with terms depending on higher-order powers of the momentum $\hat{\boldsymbol{p}}$ [49], thus resulting in sextic and higher powers of $\hat{\boldsymbol{p}}$ inside the square brackets of the effective Hamiltonian (2.3). However, as shown in Ref. [49] and discussed in the Appendix, the mapping between the real and the effective descriptions can always be arranged in such a way that these "non-geodesic" terms are proportional to the radial momentum $\hat{p}_r \equiv \boldsymbol{n}\cdot\hat{\boldsymbol{p}}$, thus vanishing for circular orbits, at all PN orders. Moreover, we will show in the Appendix that this holds true even if the mapping (2.4) between the real and the effective Hamiltonians is assumed to be valid at *all* PN orders. This standpoint was also adopted in Ref. [79], and it is the one that we embrace in this paper. In other words, our results are valid for the class of EOB models that adopt the mapping (2.4) at all PN orders, and for which the non-geodesic higher-order momentum terms are proportional to $\hat{p}_r$, thus vanishing for circular orbits.

We notice that the 3PN-accurate expression (2.2a) of the EOB potential $A(r)$ does not contain terms proportional to ν^2 and ν^3, despite the fact the PN binding energy does contain such terms. By contrast, at 3PN order, the EOB "radial" potential $B(r)$ — and hence the inverse product $\bar{D} = (AB)^{-1}$ [*cf.* Eq. (2.2b)] — contains a term proportional to ν^2. The GSF results will allow us to control the exact contributions proportional to the binary's mass ratio $q \equiv m_1/m_2 = \nu + \mathcal{O}(\nu^2)$,[3] thus *only* the terms linear in ν in $A(r)$ and $\bar{D}(r)$.

In the next two Subsections, we will derive the GSF contributions to the EOB potentials, namely the functions $A_{\rm SF}(u)$ and $\bar{D}_{\rm SF}(u)$ such that[4]

$$ A(u) = 1 - 2u + \nu\,A_{\rm SF}(u) + \mathcal{O}(\nu^2) \,, \tag{2.5a} $$

$$ \bar{D}(u) = 1 + \nu\,\bar{D}_{\rm SF}(u) + \mathcal{O}(\nu^2) \,. \tag{2.5b} $$

A. Self-force contribution to the EOB effective metric potential A

We will restrict the discussion to *circular* orbits, computing first the EOB energy $E_{\rm EOB}$ for such orbits. Now,

[3] Without any loss of generality, we assume $m_1 \leqslant m_2$.
[4] In the notations of Refs. [79, 81], we have $A_{\rm SF} = a$ and $\bar{D}_{\rm SF} = \bar{d}$.

the angular momentum $L \equiv p_\phi$ can be determined as a function of the inverse separation u by solving the equation

$$\dot{p}_r = -\frac{\partial H_{\rm EOB}}{\partial r}(r, p_r = 0, p_\phi) = 0\,, \tag{2.6}$$

which is valid for circular orbits only. From the expressions (2.3) and (2.4) of the effective and EOB Hamiltonians, this gives

$$\frac{L^2(u)}{\mu^2 M^2} = -\frac{A'(u)}{2uA(u) + u^2 A'(u)}\,, \tag{2.7}$$

where we denote $A' \equiv {\rm d}A/{\rm d}u$. Replacing this result in the expressions for the Hamiltonians, we obtain the circular-orbit EOB energy as

$$E_{\rm EOB}(u) = M\sqrt{1 + 2\nu\left(\frac{E_{\rm eff}(u)}{\mu} - 1\right)}\,, \tag{2.8a}$$

$$E_{\rm eff}(u) = \mu\sqrt{\frac{2A^2(u)}{2A(u) + uA'(u)}}\,. \tag{2.8b}$$

We also introduce the dimensionless coordinate-invariant quantity $x \equiv (M\Omega)^{2/3}$, where Ω is the constant circular-orbit frequency, given by

$$\Omega = \frac{\partial H_{\rm EOB}}{\partial p_\phi}(r, p_r = 0, p_\phi)\,, \tag{2.9}$$

as well as $r_\Omega \equiv M/x$, a convenient invariant measure of the orbital separation.

Since we are interested in improving the EOB Hamiltonian using GSF results, we will work at linear order in the symmetric mass ratio ν, thus neglecting terms $\mathcal{O}(\nu^2)$ or higher. Inverting Eq. (2.9) and making use of the expression (2.7) for the angular momentum yields [79]

$$u = x + \nu\left[\frac{x}{6}\,A'_{\rm SF}(x) + \frac{2}{3}\,x\left(\frac{1-2x}{\sqrt{1-3x}} - 1\right)\right] + \mathcal{O}(\nu^2)\,. \tag{2.10}$$

Next, we compute the (specific) EOB binding energy $\hat{E}_{\rm EOB} \equiv (E_{\rm EOB} - M)/\mu$ at linear order in ν, for circular orbits. From Eqs. (2.8), in which we substitute the coordinate-dependent variable u in favor of the invariant variable x using (2.10), we obtain

$$\hat{E}_{\rm EOB}(x) = \frac{1-2x}{\sqrt{1-3x}} - 1 + \nu\left\{\frac{1-4x}{(1-3x)^{3/2}}\frac{A_{\rm SF}(x)}{2} - \frac{x}{\sqrt{1-3x}}\frac{A'_{\rm SF}(x)}{3} - \left(\frac{1-2x}{\sqrt{1-3x}} - 1\right)\times \left[\frac{x}{3}\frac{1-6x}{(1-3x)^{3/2}} + \frac{1}{2}\left(\frac{1-2x}{\sqrt{1-3x}} - 1\right)\right]\right\} + \mathcal{O}(\nu^2)\,. \tag{2.11}$$

Recently, Ref. [87] used the first law of binary point-particle mechanics [88], together with GSF results for the redshift observable z [38, 82–85], to compute the binding energy E and total angular momentum L of a circular-orbit non-spinning compact binary, through next-to-leading order in the symmetric mass ratio ν (at all PN orders). In particular, the specific binding energy $\hat{E} \equiv E/\mu$ reads [87]

$$\hat{E}(x) = \frac{1-2x}{\sqrt{1-3x}} - 1 + \nu\left[\frac{1}{2}\,z_{\rm SF}(x) - \frac{x}{3}\,z'_{\rm SF}(x) + \sqrt{1-3x} - 1 + \frac{x}{6}\,\frac{7-24x}{(1-3x)^{3/2}}\right] + \mathcal{O}(\nu^2)\,, \tag{2.12}$$

where $z_{\rm SF}(x)$ is the self-force contribution to the redshift z of the lightest point mass, which is known numerically, with high accuracy, for circular orbits down to $r_\Omega = 5M$ (see below for more details).

By construction of the EOB model, the EOB binding energy $\hat{E}_{\rm EOB}$ must coincide with the binding energy $\hat{E}$ of the real binary system when expanded in powers of ν. Equating Eqs. (2.11) and (2.12) yields the following linear first-order ordinary differential equation for $A_{\rm SF}(x)$:

$$2x\,A'_{\rm SF}(x) - 3\frac{1-4x}{1-3x}A_{\rm SF}(x) = x\,\frac{1-6x}{1-3x} + \sqrt{1-3x}\times \left[2x\,z'_{\rm SF}(x) - 3z_{\rm SF}(x) + x\,\frac{1-5x+12x^2}{(1-3x)^2}\right]. \tag{2.13}$$

Interestingly, this differential equation can be solved analytically in terms of $z_{\rm SF}(x)$. The solution is particularly simple, and explicitly reads[5]

$$A_{\rm SF}(x) = \sqrt{1-3x}\;z_{\rm SF}(x) - x\left(1 + \frac{1-4x}{\sqrt{1-3x}}\right). \tag{2.14}$$

This is one of the most important results of this paper: we have succeeded in relating the known GSF contribution $z_{\rm SF}(x)$ in the redshift observable to the EOB dynamics for circular orbits. As a result, we can now compute the EOB radial potential $A(r)$ given in Eq. (2.5a) including *all* PN corrections, at linear order in ν. As a consistency check, the PN expansion of $z_{\rm SF}(x)$, as given by Eq. (4.16) and Table I of Ref. [88], can be used with Eq. (2.14) to recover the 3PN expansion (2.2a) of $A_{\rm SF}(x)$.

We stress that the EOB model with this form of the potential $A(r)$ automatically reproduces the shift of the ISCO frequency under the effect of the conservative part of the GSF, as calculated by Barack and Sago in Refs. [39, 80]. This is because the notion of ISCO coincides with that of minimum energy circular orbit (MECO) for any orbital dynamics that can be derived from a Hamiltonian [89], and the MECO as computed from Eq. (2.12) returns the correct ISCO frequency shift [87]. This is a considerable improvement over earlier versions of the EOB potential $A(r)$, which were resorting to free parameters regulating unknown high-order PN

[5] The homogeneous solution must vanish because the PN expansion of $A_{\rm SF}(x)$ cannot involve half-integer powers of x.

effects [53, 71, 79] in order to reproduce the ISCO frequency shift due to the conservative GSF.

Furthermore, if we use our newly derived potential $A(r)$ together with Eqs. (2.7) and (2.10) to compute the dimensionless angular momentum $\hat{L} \equiv L/(\mu M)$ for circular orbits, expressed in terms of the coordinate-invariant quantity x, we recover the result obtained in Ref. [87], namely

$$\hat{L}(x) = \frac{1}{\sqrt{x(1-3x)}} + \nu \left[-\frac{1}{3\sqrt{x}}\, z'_{\rm SF}(x) + \frac{1}{6\sqrt{x}} \frac{4-15x}{(1-3x)^{3/2}} \right] + \mathcal{O}(\nu^2)\,, \qquad (2.15)$$

which holds at all PN orders and at linear order in ν. This comes at no surprise because the binding energy and total angular momentum for circular orbits satisfy the exact relation $\partial \hat{E}/\partial \hat{L} = M\Omega$ in the EOB model. Therefore, once the energy coincides with the exact expression established in Ref. [87], so must the angular momentum.

The GSF contribution $z_{\rm SF}(x)$ to the redshift observable has been calculated numerically in Refs. [38, 82–85] for a variety of orbital separations, in the range $5M \leqslant r_\Omega \leqslant 500M$. In the companion paper [87], we established that this numerical data can conveniently be represented with an accuracy better than a part in 10^5, using the compact analytical formula

$$z_{\rm SF}(x) = 2x\, \frac{1 + a_1 x + a_2 x^2}{1 + a_3 x + a_4 x^2 + a_5 x^3}\,, \qquad (2.16)$$

with the coefficients $a_1 = -2.18522$, $a_2 = 1.05185$, $a_3 = -2.43395$, $a_4 = 0.400665$, and $a_5 = -5.9991$. This fitting formula accounts for the leading-order (1PN) behavior $z_{\rm SF}(x) = 2x + \mathcal{O}(x^2)$ when $x \to 0$ [88]. Since current GSF data for $z_{\rm SF}(x)$ is limited to orbital separations $r_\Omega \geqslant 5M$, the GSF-accurate EOB potential $A(u)$ given by Eqs. (2.5a) and (2.14) is (for now) only known in the range $0 \leqslant x \leqslant 1/5$.

B. Self-force contribution to the EOB effective metric potential $\bar{D}$

The non-circular conservative dynamics of spinless binaries is regulated by the radial frequency Ω_r and by the averaged angular frequency Ω_ϕ, respectively defined by

$$\Omega_r \equiv \frac{2\pi}{P}\,, \qquad (2.17a)$$

$$\Omega_\phi \equiv \frac{1}{P} \int_0^P \dot{\phi}(t)\, {\rm d}t = K\, \Omega_r\,, \qquad (2.17b)$$

where P is the radial period, namely the time interval between two successive periastron passages, $\dot{\phi} \equiv {\rm d}\phi/{\rm d}t$ is the time derivative of the orbital phase $\phi(t)$, and $\Delta\Phi/(2\pi) = K - 1$ is the fractional advance of the periastron per radial period. In the circular-orbit limit, by definition the radial frequency vanishes at the ISCO; hence the periastron advance $K = \Omega_\phi/\Omega_r$ blows up there. For this reason, Refs. [79, 81] found it convenient to work with the quantity $W \equiv 1/K^2$, which is regular at the ISCO. Reference [81] calculated numerically the GSF contribution to W, *i.e.* the function $\rho_{\rm SF}(x)$ such that

$$W(x) = 1 - 6x + \nu\, \rho_{\rm SF}(x) + \mathcal{O}(\nu^2)\,. \qquad (2.18)$$

The authors performed several fits of the GSF data for $\rho_{\rm SF}(x)$ (in the range $6M \leqslant r_\Omega \leqslant 80M$). In particular, they found that this data can be accurately reproduced at the 2.4×10^{-3} level by means of the compact analytic formula

$$\rho_{\rm SF}(x) = 14x^2\, \frac{1 + b_1\, x}{1 + b_2\, x + b_3\, x^2}\,, \qquad (2.19)$$

with $b_1 = 13.3687$, $b_2 = 4.60958$, and $b_3 = -9.47696$. (Using a denser data set in a more limited frequency range, Ref. [90] later found that the values $b_1 = 12.9906$, $b_2 = 4.57724$, and $b_3 = -10.3124$ yield a fit accurate at the 10^{-5} level.) As with Eq. (2.16), the fitting formula (2.19) accounts for the leading-order (2PN) behavior of $\rho_{\rm SF}(x)$ when $x \to 0$ [81].

Reference [79] recently studied the dynamics of slightly eccentric orbits within the EOB formalism, and found that the GSF correction $\rho_{\rm SF}(x)$ to the periastron advance is related to the EOB potentials $A_{\rm SF}(x)$ and $\bar{D}_{\rm SF}(x)$ by[6]

$$\rho_{\rm SF}(x) = 4x \left(1 - \frac{1-2x}{\sqrt{1-3x}} \right) + A_{\rm SF}(x) + x\, A'_{\rm SF}(x) + \frac{x}{2}\,(1-2x)\, A''_{\rm SF}(x) + (1-6x)\, \bar{D}_{\rm SF}(x)\,. \qquad (2.20)$$

Solving the above equation for the unknown $\bar{D}_{\rm SF}(x)$, we immediately obtain

$$\bar{D}_{\rm SF}(x) = \frac{1}{1-6x} \left[\rho_{\rm SF}(x) + 4x \left(\frac{1-2x}{\sqrt{1-3x}} - 1 \right) - A_{\rm SF}(x) - x\, A'_{\rm SF}(x) - \frac{x}{2}\,(1-2x)\, A''_{\rm SF}(x) \right], \qquad (2.21)$$

where $A_{\rm SF}(x)$ is given explicitly in terms of $z_{\rm SF}(x)$ by Eq. (2.14) above. Equation (2.21) is another important result of this paper: the EOB potential $\bar{D}(r)$ governing the *non-radial* motion, as given by Eq. (2.5b), is now known exactly at linear order in ν, through the known GSF contributions $z_{\rm SF}(x)$ and $\rho_{\rm SF}(x)$ to the redshift observable and periastron advance.

Note that the apparent pole at the Schwarzschild ISCO ($x = 1/6$) in Eq. (2.21) must be canceled out by a factor $(1-6x)$ in the numerator, because the potential $\bar{D}(r)$ is

[6] This result requires that the quartic power in the radial momentum p_r inside the square brackets of Eq. (2.3) be neglected. This is correct in the limit of small eccentricity $e \ll 1$, for which $p_r \sim e$; see Ref. [79] for more details.

perfectly regular at the ISCO. This can be verified using the fit (2.16) for $z_{\rm SF}(x)$, which is accurate to within 10^{-5}, together with the fit (2.19) for $\rho_{\rm SF}(x)$, which is accurate to within 2.4×10^{-3} using the coefficients b_1, b_2 and b_3 from Ref. [81], and to within 10^{-5}, although in a more limited frequency range, using the coefficients b_1, b_2 and b_3 from Ref. [90]. Using these fits, the behavior of $\bar{D}_{\rm SF}(x)$ near the ISCO is of the form $\bar{D}_{\rm SF}(x)=\epsilon/(x-1/6)+\mathcal{O}(1)$, where the dimensionless parameter ϵ is about 4×10^{-5} with the coefficients b_1, b_2 and b_3 from Ref. [81], and 3.4×10^{-5} with the coefficients b_1, b_2 and b_3 from Ref. [90]. One can therefore argue that the value of ϵ is comparable to the accuracy of the fits and thus compatible with zero.

Finally, when using the known PN expansions of the GSF contributions $\rho_{\rm SF}(x)$ and $z_{\rm SF}(x)$ to the redshift observable and periastron advance (see *e.g.* Eqs. (5.32) and (5.39) of Ref. [79], and Eq. (4.16) and Table I of Ref. [88]), we recover, as expected, the 3PN expansion (2.2b) of $\bar{D}_{\rm SF}(x)$.

III. HIGH-ORDER POST-NEWTONIAN TERMS IN THE EOB POTENTIALS

Recently, the authors of Ref. [88] derived a first law of mechanics for non-spinning compact objects modelled as point particles, and moving along exactly circular orbits. By making use of previous GSF results for the redshift observable [38, 84, 85], they could determine the numerical values of some previously unknown coefficients entering the expression of the circular-orbit binding energy E. Through 6PN order, the (specific) binding energy explicitly reads

$$\hat{E}(x)=-\frac{x}{2}\left\{1+\left(-\frac{3}{4}-\frac{\nu}{12}\right)x+\left(-\frac{27}{8}+\frac{19}{8}\nu-\frac{\nu^2}{24}\right)x^2+\left(-\frac{675}{64}+\left[\frac{34445}{576}-\frac{205}{96}\pi^2\right]\nu\right.\right.$$
$$\left.-\frac{155}{96}\nu^2-\frac{35}{5184}\nu^3\right)x^3+\left(-\frac{3969}{128}+\nu\,e_4(\nu)+\frac{448}{15}\nu\,\ln x\right)x^4+\left(-\frac{45927}{512}+\nu\,e_5(\nu)$$
$$\left.+\left[-\frac{4988}{35}-\frac{1904}{15}\nu\right]\nu\,\ln x\right)x^5+\left(-\frac{264627}{1024}+\nu\,e_6(\nu)+\nu\,e_6^{\ln}(\nu)\,\ln x\right)x^6+o(x^6)\Big\}\,, \tag{3.1}$$

where the numerical values of the 4PN, 5PN and 6PN coefficients $e_4(0)$, $e_5(0)$, $e_6(0)$, and $e_6^{\ln}(0)$ were found to be [88]

$$e_4(0)=+153.8803(1)\,, \tag{3.2a}$$
$$e_5(0)=-55.13(3)\,, \tag{3.2b}$$
$$e_6(0)=+588(7)\,, \tag{3.2c}$$
$$e_6^{\ln}(0)=-1144(2)\,. \tag{3.2d}$$

(The uncertainty in the last digit is indicated in parenthesis.) Note that the leading-order 4PN and next-to-leading order 5PN logarithmic contributions to the binding energy are known analytically [85]. The value of the post-GSF coefficient (term $\propto\nu^2$) in the 5PN logarithmic contribution is that corresponding to the "physical problem" in the language of Ref. [88], *i.e.* when the helical symmetry is *not* imposed (see [88] for more details).

In the next two Subsections, we will use Eqs. (3.1) and (3.2), together with the results of Ref. [81], to compute the 4PN, 5PN and 6PN coefficients in $A(u)$, as well as the 4PN and 5PN coefficients in $\bar{D}(u)$, at linear order in the symmetric mass ratio ν.

A. High-order post-Newtonian terms in the EOB metric potential A

Similarly to what was done in Sec. II, we restrict here to the class of EOB models that adopt the mapping (2.4) at all PN orders, and for which the non-geodesic higher-order momentum terms are proportional to the radial momentum. As a consequence, the 4PN, 5PN and 6PN corrections determined in Eqs. (3.1) and (3.2) enter the effective Hamiltonian only through the radial potential $A(r)$, *i.e.*, through the coefficients $a_5(\nu)$, $a_5^{\ln}(\nu)$, $a_6(\nu)$, $a_6^{\ln}(\nu)$, $a_7(\nu)$ and $a_7^{\ln}(\nu)$ in the PN expansion

$$A(u)=1-2u+2\nu\,u^3+\left(\frac{94}{3}-\frac{41\pi^2}{32}\right)\nu\,u^4$$
$$+\nu\left[a_5(\nu)+a_5^{\ln}(\nu)\,\ln u\right]u^5$$
$$+\nu\left[a_6(\nu)+a_6^{\ln}(\nu)\,\ln u\right]u^6$$
$$+\nu\left[a_7(\nu)+a_7^{\ln}(\nu)\,\ln u\right]u^7+o(u^7)\,. \tag{3.3}$$

A comment regarding the general structure of the PN expansion of $A(u)$ is in order. It was argued in Ref. [85] that terms involving powers of logarithms should not occur in the *conservative* part of the dynamics of a compact binary system before the very high 7PN order. Within the class of EOB Hamiltonians that we consider in this work, the potential A is directly related to the conserved binding energy E of the real binary system. Hence we

expect no term of the type $(\ln u)^p$, with $p \geqslant 2$, in the 6PN-accurate expansion (3.3) of $A(u)$.

Now, in order to derive the $\nu \to 0$ limits of the coefficients $a_i(\nu)$ and $a_i^{\ln}(\nu)$ (with $i = 5, 6, 7$), we first determine the angular momentum $L = p_\phi$ as a function of the circular-orbit frequency Ω by solving Eqs. (2.6) and (2.9). Second, we insert $L = L(\Omega)$ in Eqs. (2.3) and (2.4), set $p_r = 0$, and expand Eq. (2.4) in PN orders. Third, after subtracting the rest-mass contribution, we equate the result to Eq. (3.1), and finally obtain

$$a_5(0) = -\frac{275\,139}{4\,480} + \frac{3}{7}\,e_4(0) + \frac{123}{64}\pi^2\,, \tag{3.4a}$$

$$a_5^{\ln}(0) = \frac{64}{5}\,, \tag{3.4b}$$

$$a_6(0) = -\frac{2\,772\,125}{96\,768} - \frac{9}{14}\,e_4(0) + \frac{1}{3}\,e_5(0) + \frac{369}{256}\pi^2\,, \tag{3.4c}$$

$$a_6^{\ln}(0) = -\frac{7\,004}{105}\,, \tag{3.4d}$$

$$a_7(0) = -\frac{23\,821\,223}{322\,560} - \frac{27}{56}\,e_4(0) - \frac{1}{2}e_5(0) + \frac{3}{11}\,e_6(0) - \frac{6}{121}\,e_6^{\ln}(0) + \frac{1\,107}{512}\pi^2\,, \tag{3.4e}$$

$$a_7^{\ln}(0) = \frac{398}{7} + \frac{3}{11}\,e_6^{\ln}(0)\,. \tag{3.4f}$$

Note that the values of the 4PN and 5PN log-coefficients $a_5^{\ln}(0)$ and $a_6^{\ln}(0)$ are known analytically.[7] Using the numerical results (3.2) for the binding energy, we find for the other 4PN, 5PN and 6PN unknown coefficients:

$$a_5(0) = +23.50190(5)\,, \tag{3.5a}$$

$$a_6(0) = -131.72(1)\,, \tag{3.5b}$$

$$a_7(0) = +118(2)\,, \tag{3.5c}$$

$$a_7^{\ln}(0) = -255.0(5)\,. \tag{3.5d}$$

As a consistency check, we verified that the same values for these coefficients also follow from expanding in PN orders the potential A given by Eqs. (2.5a) and (2.14), using the 6PN-accurate fit to $z_{\rm SF}(x)$ given in Eq. (4.16) and Table II of Ref. [88].

Finally, we note that the values of the coefficients $a_5(0)$ and $a_6(0)$, as determined in Ref. [79] [see Eq. (4.46) there] by combining the EOB/NR comparison of Ref. [70] with the constraint coming from the GSF calculation of the ISCO frequency shift, are in poor agreement with the exact results (3.5a) and (3.5b); in particular the signs of both coefficients are wrongly predicted. Even without taking into account the constraint from the GSF, the correct values (3.5a) and (3.5b) lie far outside the (banana-shaped) region of the $a_5(0), a_6(0)$ plane favored by a comparison of the EOB prediction with the NR waveform of an equal-mass binary black-hole simulation [70, 91]. This disagreement does not surprise us. Indeed, several causes can affect the correct values of the coefficients $a_5(0)$ and $a_6(0)$ when they are extracted from a EOB/NR calibration, such as radiation-reaction effects and all higher-order PN contributions in $A(r)$, which become important during the plunge and close to merger, but are neglected in those calibrations.

[7] Actually these logarithmic terms are known for *all* mass ratios: $a_5^{\ln}(\nu) = \frac{64}{5}$ and $a_6^{\ln}(\nu) = -\frac{7\,004}{105} - \frac{144}{5}\,\nu$.

B. High-order post-Newtonian terms in the EOB metric potential $\bar{D}$

We will now show that by combining the results of this paper with those of Ref. [81], we can also determine the exact or approximate numerical values of the non-logarithmic and logarithmic coefficients $\bar{d}_4(\nu)$, $\bar{d}_5(\nu)$, $\bar{d}_4^{\ln}(\nu)$ and $\bar{d}_5^{\ln}(\nu)$ appearing at 4PN and 5PN order in the potential $\bar{D}$:

$$\bar{D}(u) = 1 + 6\nu\,u^2 + (52 - 6\nu)\,\nu\,u^3 + \nu\left[\bar{d}_4(\nu) + \bar{d}_4^{\ln}(\nu)\,\ln u\right] u^4 + \nu\left[\bar{d}_5(\nu) + \bar{d}_5^{\ln}(\nu)\,\ln u\right] u^5 + o(u^5)\,. \tag{3.6}$$

The authors of Ref. [81] extracted numerically some unknown high-order PN terms in the function $\rho_{\rm SF}(x)$, and used the relation (2.20) between $\rho_{\rm SF}$, $A_{\rm SF}$, and $\bar{D}_{\rm SF}$ to put constraints on some unknown high-order PN coefficients appearing in the EOB potentials $A(u)$ and $\bar{D}(u)$. In particular, Ref. [81] derived the following constraints on the $\nu \to 0$ limit of the PN coefficients $\bar{d}_4(\nu)$ and $\bar{d}_5(\nu)$:

$$10\,a_5(0) + \bar{d}_4(0) + \frac{9}{2}\,a_5^{\ln}(0) = 518.6^{+7}_{-4}\,, \tag{3.7a}$$

$$14\,a_5(0) + 6\,\bar{d}_4(0) - 15\,a_6(0) - \bar{d}_5(0) + 8\,a_5^{\ln}(0) - \frac{11}{2}\,a_6^{\ln}(0) = 4779^{-400}_{+1200}\,, \tag{3.7b}$$

as well as the following exact relations between the $\nu \to 0$ limit of the PN coefficients $\bar{d}_4^{\ln}(\nu)$ and $\bar{d}_5^{\ln}(\nu)$:

$$10\,a_5^{\ln}(0) + \bar{d}_4^{\ln}(0) = \frac{2\,512}{15}\,, \tag{3.8a}$$

$$14\,a_5^{\ln}(0) - 15\,a_6^{\ln}(0) + 6\,\bar{d}_4^{\ln}(0) - \bar{d}_5^{\ln}(0) = \frac{11\,336}{7}\,. \tag{3.8b}$$

Substituting Eqs. (3.4b), (3.4d), and (3.5) in the above equations, we get

$$\bar{d}_4(0) = +226.0^{+7}_{-4}\,, \tag{3.9a}$$

$$\bar{d}_4^{\ln}(0) = +\frac{592}{15}\,, \tag{3.9b}$$

$$\bar{d}_5(0) = -649^{-1200}_{+400}\,, \tag{3.9c}$$

$$\bar{d}_5^{\ln}(0) = -\frac{1420}{7}\,. \tag{3.9d}$$

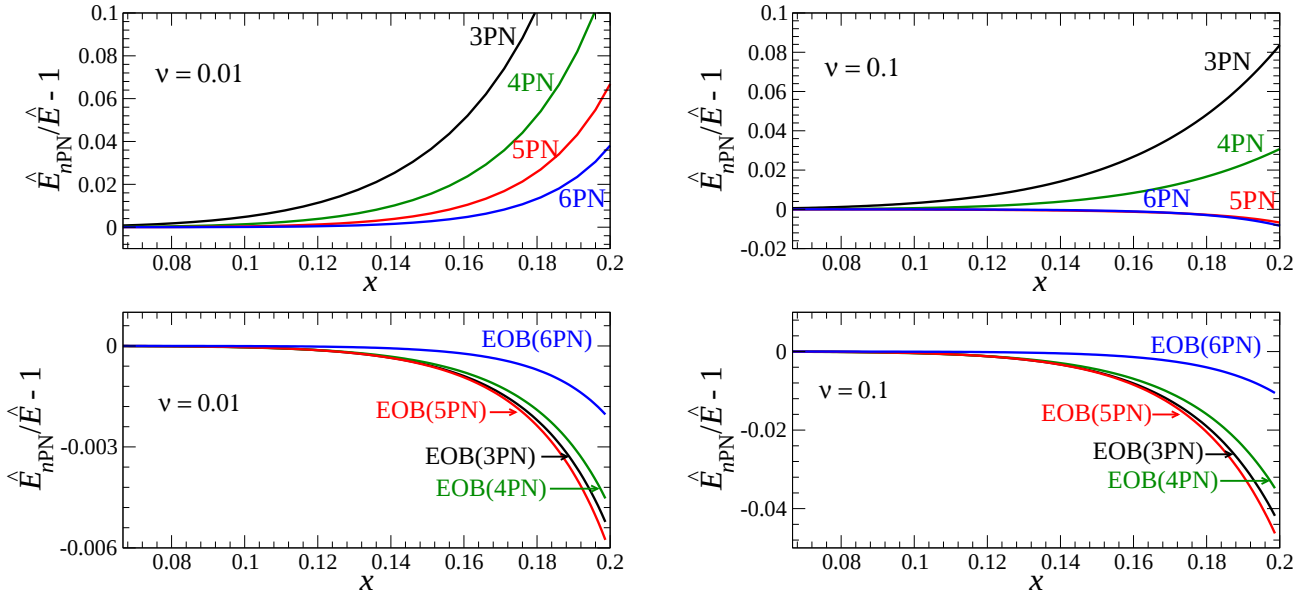

FIG. 1: The fractional difference between the GSF-accurate (specific) binding energy and the (specific) binding energy calculated at linear order in ν using standard PN approximants (upper plot), and EOB approximants (lower plot), for $\nu = 0.01$ (left panel) and $\nu = 0.1$ (right panel).

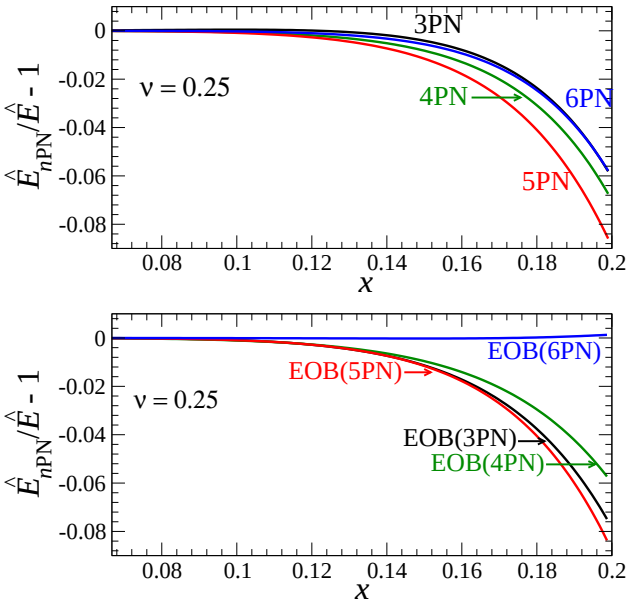

FIG. 2: Same as in Fig. 1, for an equal-mass binary ($\nu = 0.25$).

As a consistency check, we verified that the values (3.9) can be recovered by inserting the PN fits to $z_{\rm SF}(x)$ and $\rho_{\rm SF}(x)$ given in Refs. [81, 88] into the exact expression (2.5b) and (2.21) for $\bar{D}$.

In summary, building on the results of Refs. [81, 88], we have computed the 4PN, 5PN and 6PN terms in the EOB potential $A(u)$, as well as the 4PN and 5PN terms in the potential $\bar{D}(u)$, at linear order in ν.

IV. DISCUSSION AND CONCLUSIONS

The potential $A(u)$ given by Eqs. (2.5a) and (2.14) ensures that the EOB binding energy for circular orbits coincides, at linear order in ν, with the exact result (2.12). In order to investigate the properties of the EOB resummation, as opposed to the standard PN expansion, we will here compare this exact result for the binding energy to the PN predictions, as well as to the EOB binding energy, as computed with the PN-expanded version of the potential $A(u)$ [*cf.* Eq. (3.3)].

In Figs. 1 and 2 we show the fractional difference between the GSF-accurate (specific) binding energy $\hat{E}(x)$ given by Eq. (2.12), and either the EOB (specific) binding energy obtained from Eqs. (2.8) using the PN-expanded potential A (at linear order in ν), or the PN (specific) binding energy given in Eq. (3.1), including only the terms linear in ν. The fractional difference is presented as a function of $x = (M\Omega)^{2/3}$ up to $x = 1/5$. We consider three representative symmetric mass ratios, namely $\nu = 0.01, 0.1$, and 0.25, and several PN orders.[8]

From Figs. 1 and 2 we observe that up to $x = 1/5$ the EOB-approximants are much closer than the PN-approximants to the exact GSF result for the small mass-ratio case $\nu = 0.01$, and are (roughly) comparable, with some differences depending on the PN order, to the exact

[8] In order to express the EOB binding energy (2.8) at nPN order as a function of x rather than u, we insert Eq. (2.7) into the relation $x^{3/2} = M\partial H_{\rm EOB}/\partial L(r = 1/u, p_r = 0, L)$, and invert the latter to obtain u as a PN expansion in x.

GSF result for the comparable mass-ratio cases $\nu = 0.1$ and $\nu = 0.25$.

These results confirm the utility of resumming the PN dynamics around the test-mass limit if the goal is to obtain a flexible model that can smoothly *bridge* between the test-mass and equal-mass limits. This flexibility exists in the EOB model not only at the level of the binding energy for circular orbits, but more importantly at the level of the Hamiltonian, thus for generic orbits and beyond the innermost stable circular orbit. It is a crucial feature that has allowed to build faithful inspiral-merger-ringdown templates that can span the entire binary's mass-ratio range [57, 60–78].

We leave to future work a detailed study of how the EOB model, augmented with the gravitational self-force results in $A(u)$ and $\bar{D}(u)$, performs against numerical-relativity simulations of comparable-mass black-hole binaries [71]. Comparisons using a 4PN, 5PN, or even 6PN-accurate EOB model can already be pursued. However, in order to use the EOB potentials with all PN terms linear in ν, more self-force data is needed for the redshift observable $z_{\rm SF}(x)$ beyond $x = 1/5$, and for the periastron advance $\rho_{\rm SF}(x)$ beyond $x = 1/6$.

Acknowledgments

All three authors acknowledge support from NSF Grant No. PHY-0903631. A.B. also acknowledges support from NASA Grant No. NNX09AI81G, and A.L.T. from the Maryland Center for Fundamental Physics.

Appendix A: On the generic structure of the effective-one-body Hamiltonian

Following Ref. [49], but including also the logarithmic contributions that were left out of their analysis, we show that it is possible to build EOB Hamiltonians such that (i) the mapping (2.4) holds at all PN orders and (ii) the non-geodesic terms in the square brackets of Eq. (2.3) are proportional to the radial momentum, at all PN orders, thus vanishing for circular orbits.

We start by considering the generic structure of the (specific) two-body Hamiltonian in the center-of-mass frame, at a given PN order, as a function of the reduced canonical variables $\hat{\boldsymbol{p}} = \boldsymbol{p}/\mu$ and $\boldsymbol{q} = \boldsymbol{r}/M$:

$$\begin{aligned}\widehat{H}_{(n,k)\rm PN}(\boldsymbol{r},\boldsymbol{p}) = (\ln q)^k \Bigg\{ & \hat{p}^{2(n+1)} \\ & + \frac{1}{q}\left[\hat{p}^{2n} + \hat{p}^{2n-2}(n\hat{p})^2 + \cdots + (n\hat{p})^{2n}\right] \\ & + \frac{1}{q^2}\left[\hat{p}^{2(n-1)} + \cdots + (n\hat{p})^{2(n-1)}\right] \\ & + \cdots + \frac{1}{q^{n+1}}\Bigg\}, \end{aligned} \tag{A1}$$

where we introduce the notations $q \equiv \sqrt{\boldsymbol{q}\cdot\boldsymbol{q}}$ and $(n\hat{p}) \equiv \boldsymbol{n}\cdot\hat{\boldsymbol{p}}$, and where we use a subscript (n,k)PN to denote the contribution to the nPN-accurate Hamiltonian which is $\mathcal{O}(c^{-2n})$ and proportional to $(\ln q)^k$, with $k \geqslant 0$. Indeed, the general structure of the near-zone expansion (formally $r/c \to 0$) of the PN metric is known to be of the type $[\ln(r/c)]^k (r/c)^n$ [92], yielding terms proportional to $(\ln q)^k$ in the conservative dynamics starting at 4PN order [93] (see also [85] for a more recent discussion).

The number of independent coefficients in the Hamiltonian (A1) is easily found to be [49]

$$C_{\rm H}(n,k) = \frac{(n+1)(n+2)}{2} + 1\,. \tag{A2}$$

The mapping of the real Hamiltonian onto the effective Hamiltonian can be achieved through a canonical transformation [47, 49]. The most general generating function reads

$$\begin{aligned} G_{(n,k)\rm PN}(\boldsymbol{r},\boldsymbol{p}) = (\ln q)^k\,(\boldsymbol{r}\cdot\boldsymbol{p}) \Bigg\{ & \hat{p}^{2n} + \frac{1}{q}\Big[\hat{p}^{2(n-1)} \\ & + \cdots + (n\hat{p})^{2(n-1)}\Big] + \cdots + \frac{1}{q^n}\Bigg\}. \end{aligned} \tag{A3}$$

Thus, the number of independent coefficients in the generating function is [49]

$$C_{\rm G}(n,k) = \frac{n(n+1)}{2} + 1\,. \tag{A4}$$

At 3PN or higher orders, non-geodesic (NG) terms resulting in quartic or higher powers of the momentum $\hat{\boldsymbol{p}}$ can appear inside the square brackets of the effective Hamiltonian (2.3). At 3PN order, the NG terms symbolically read

$$\mathcal{Q}_{\rm 3PN}(\boldsymbol{r},\boldsymbol{p}) = \frac{1}{q^2}\left[\hat{p}^4 + \hat{p}^2\,(n\hat{p})^2 + (n\hat{p})^4\right]. \tag{A5}$$

(The first logarithms appear at 4PN order.) At higher PN orders ($n > 3$), the generic structure is

$$\begin{aligned} \mathcal{Q}_{(n,k)\rm PN}(\boldsymbol{r},\boldsymbol{p}) = (\ln q)^k \Bigg\{ & \frac{1}{q^2}\left[\hat{p}^{2n-2} + \hat{p}^{2n-4}\,(n\hat{p})^2\right. \\ & \left. + \cdots + (n\hat{p})^{2n-2}\right] + \cdots + \\ & \frac{1}{q^{n-1}}\left[\hat{p}^4 + \hat{p}^2\,(n\hat{p})^2 + (n\hat{p})^4\right]\Bigg\}. \end{aligned} \tag{A6}$$

It is straightforward to derive that the number of arbitrary coefficients in $\mathcal{Q}_{(n,k)\rm PN}$ is

$$C_{\rm NG}(n,k) = \frac{(n+3)(n-2)}{2}\,, \tag{A7}$$

hence the number of NG terms that depend on the radial momentum $(n\hat{p})$ is

$$C^{\rm circ}_{\rm NG}(n,k) = C_{\rm NG}(n,k) - (n-2) = \frac{(n+1)(n-2)}{2}\,. \tag{A8}$$

Given that at the PN order (n,k) we have two new coefficients in the effective metric potentials A and $\bar{D}$, multiplied respectively by $u^{n+1}(\ln u)^k$ and $u^n(\ln u)^k$, but no new coefficient in the mapping between the real and effective Hamiltonians, because we assume that (2.4) is valid at all PN orders, we obtain that the difference between the number of equations to satisfy and the number of unknowns is

$$\begin{aligned}\delta(n,k) &= C_{\rm H}(n,k) - C_{\rm G}(n,k) - 2 - C^{\rm circ}_{\rm NG}(n,k)\\ &= -\frac{n\,(n-3)}{2}\,, \end{aligned} \tag{A9}$$

which is always zero or negative starting at 3PN ($n=3$). This proves that for all $n \geqslant 3$ (and any $k \geqslant 0$), it is possible to build the mapping between the real and the effective descriptions in such a way that Eq. (2.4) holds, and circular orbits follow from a "geodesic" effective Hamiltonian [*i.e.*, all the higher-momentum terms inside the square brackets in Eq. (2.3) can be chosen to be proportional to the radial momentum $(n\hat{p})$]. It is for this class of EOB Hamiltonians that we have determined the effective metric potentials A and $\bar{D}$ at all PN orders, linearly in the symmetric mass ratio ν.

[1] A. Einstein, Sitzber. Preuss. Akad. Wiss. p. 831 (1915).
[2] L. Blanchet, Living Rev. Rel. **9**, 4 (2006), arXiv:gr-qc/0202016.
[3] T. Damour, P. Jaranowski, and G. Schäfer, Phys. Lett. B **513**, 147 (2001), arXiv:gr-qc/0105038.
[4] L. Blanchet, T. Damour, and G. Esposito-Farèse, Phys. Rev. D **69**, 124007 (2004), arXiv:gr-qc/0311052.
[5] L. Blanchet, T. Damour, G. Esposito-Farèse, and B. R. Iyer, Phys. Rev. D **71**, 124004 (2005), arXiv:gr-qc/0503044.
[6] L. E. Kidder, Phys. Rev. D **77**, 044016 (2008), arXiv:0710.0614 [gr-qc].
[7] L. Blanchet, G. Faye, B. R. Iyer, and S. Sinha, Class. Quant. Grav. **25**, 165003 (2008), arXiv:0802.1249 [gr-qc].
[8] K. G. Arun, L. Blanchet, B. R. Iyer, and S. Sinha, Phys. Rev. D **80**, 124018 (2009), arXiv:0908.3854 [gr-qc].
[9] L. E. Kidder, Phys. Rev. D **52**, 821 (1995), arXiv:gr-qc/9506022.
[10] L. Blanchet, A. Buonanno, and G. Faye, Phys. Rev. D **74**, 104034 (2006), *Errata:* Phys. Rev. D **75**, 049903(E) (2007) & Phys. Rev. D **81**, 089901(E) (2010), arXiv:gr-qc/0605140.
[11] L. Blanchet, A. Buonanno, and G. Faye, Phys. Rev. D **84**, 064041 (2011), arXiv:1104.5659 [gr-qc].
[12] T. Damour, P. Jaranowski, and G. Schäfer, Phys. Rev. D **77**, 064032 (2008), arXiv:0711.1048 [gr-qc].
[13] J. Steinhoff, S. Hergt, and G. Schäfer, Phys. Rev. D **77**, 081501(R) (2008), arXiv:0712.1716 [gr-qc].
[14] J. Steinhoff, S. Hergt, and G. Schäfer, Phys. Rev. D **78**, 101503(R) (2008), arXiv:0809.2200 [gr-qc].
[15] S. Hergt and G. Schäfer, Phys. Rev. D **78**, 124004 (2008), arXiv:0809.2208 [gr-qc].
[16] J. Hartung and J. Steinhoff, Ann. Phys. **523**, 919 (2011), arXiv:1107.4294 [gr-qc].
[17] G. Faye, L. Blanchet, and A. Buonanno, Phys. Rev. D **74**, 104033 (2006), *Errata:* Phys. Rev. D **75**, 049903(E) (2007) & Phys. Rev. D **81**, 089901(E) (2010), arXiv:gr-qc/0605139.
[18] W. D. Goldberger and I. Z. Rothstein, Phys. Rev. D **73**, 104029 (2006), arXiv:hep-th/0409156.
[19] S. Foffa and R. Sturani, Phys. Rev. D **84**, 044031 (2011), arXiv:1104.1122 [gr-qc].
[20] R. A. Porto, A. Ross, and I. Z. Rothstein, JCAP **1103**, 009 (2011), arXiv:1007.1312 [gr-qc].
[21] R. A. Porto and I. Z. Rothstein, Phys. Rev. Lett. **97**, 021101 (2006), arXiv:gr-qc/0604099.
[22] R. A. Porto, Phys. Rev. D **73**, 104031 (2006), arXiv:gr-qc/0511061.
[23] R. A. Porto and I. Z. Rothstein, Phys. Rev. D **78**, 044012 (2008), *Errata:* Phys. Rev. D **81**, 029904(E) (2010) & Phys. Rev. D **81**, 029905(E) (2010), arXiv:0802.0720 [gr-qc].
[24] R. A. Porto and I. Z. Rothstein, Phys. Rev. D **78**, 044013 (2008), *Errata:* Phys. Rev. D **81**, 029904(E) (2010) & Phys. Rev. D **81**, 029905(E) (2010), arXiv:0804.0260 [gr-qc].
[25] R. A. Porto, Class. Quant. Grav. **27**, 205001 (2010), arXiv:1005.5730 [gr-qc].
[26] M. Levi, Phys. Rev. D **82**, 064029 (2010), arXiv:0802.1508 [gr-qc].
[27] M. Levi (2011), arXiv:1107.4322 [gr-qc].
[28] K. Schwarzschild, Sitzber. Preuss. Akad. Wiss. p. 189 (1916), translated in English by S. Antoci and A. Loinger, arXiv:physics/9905030.
[29] K. Schwarzschild, Sitzber. Preuss. Akad. Wiss. p. 424 (1916), translated in English by S. Antoci, arXiv:physics/9912033.
[30] R. P. Kerr, Phys. Rev. Lett. **11**, 237 (1963).
[31] E. Poisson, A. Pound, and I. Vega, Living Rev. Rel. **14**, 7 (2011), arXiv:1102.0529 [gr-qc].
[32] Y. Mino, M. Sasaki, and T. Tanaka, Phys. Rev. D **55**, 3457 (1997), arXiv:gr-qc/9606018.
[33] T. C. Quinn and R. M. Wald, Phys. Rev. D **56**, 3381 (1997), arXiv:gr-qc/9610053.
[34] T. Regge and J. A. Wheeler, Phys. Rev. **108**, 1063 (1957).
[35] F. J. Zerilli, Phys. Rev. Lett. **24**, 737 (1970).
[36] S. A. Teukolsky, Phys. Rev. Lett. **29**, 1114 (1972).
[37] S. A. Teukolsky, Astrophys. J. **185**, 635 (1973).
[38] S. Detweiler, Phys. Rev. D **77**, 124026 (2008), arXiv:0804.3529 [gr-qc].
[39] L. Barack and N. Sago, Phys. Rev. Lett. **102**, 191101 (2009), arXiv:0902.0573 [gr-qc].
[40] L. Barack and N. Sago, Phys. Rev. D **83**, 084023 (2011), arXiv:1101.3331 [gr-qc].
[41] F. Pretorius, Phys. Rev. Lett. **95**, 121101 (2005), arXiv:gr-qc/0507014.
[42] M. Campanelli, C. O. Lousto, P. Marronetti, and Y. Zlochower, Phys. Rev. Lett. **96**, 111101 (2006), arXiv:gr-qc/0511048.
[43] J. G. Baker, J. Centrella, D.-I. Choi, M. Koppitz, and J. van Meter, Phys. Rev. Lett. **96**, 111102 (2006),

arXiv:gr-qc/0511103.
[44] C. O. Lousto and Y. Zlochower, Phys. Rev. Lett. **106**, 041101 (2011), arXiv:1009.0292 [gr-qc].
[45] G. Lovelace, M. A. Scheel, and B. Szilágyi, Phys. Rev. D **83**, 024010 (2011), arXiv:1010.2777 [gr-qc].
[46] G. Lovelace, M. Boyle, M. A. Scheel, and B. Szilágyi, Class. Quant. Grav. **29**, 045003 (2012), arXiv:1110.2229 [gr-qc].
[47] A. Buonanno and T. Damour, Phys. Rev. D **59**, 084006 (1999), arXiv:gr-qc/9811091.
[48] E. Brezin, C. Itzykson, and J. Zinn-Justin, Phys. Rev. D **1**, 2349 (1970).
[49] T. Damour, P. Jaranowski, and G. Schäfer, Phys. Rev. D **62**, 084011 (2000), arXiv:gr-qc/0005034.
[50] T. Damour, Phys. Rev. D **64**, 124013 (2001), arXiv:gr-qc/0103018.
[51] T. Damour, P. Jaranowski, and G. Schäfer, Phys. Rev. D **78**, 024009 (2008), arXiv:0803.0915 [gr-qc].
[52] E. Barausse, E. Racine, and A. Buonanno, Phys. Rev. D **80**, 104025 (2009), arXiv:0907.4745 [gr-qc].
[53] E. Barausse and A. Buonanno, Phys. Rev. D **81**, 084024 (2010), arXiv:0912.3517 [gr-qc].
[54] E. Barausse and A. Buonanno, Phys. Rev. D **84**, 104027 (2011), arXiv:1107.2904 [gr-qc].
[55] A. Nagar, Phys. Rev. D **84**, 084028 (2011), arXiv:1106.4349 [gr-qc].
[56] A. Buonanno and T. Damour, Phys. Rev. D **62**, 064015 (2000), arXiv:gr-qc/0001013.
[57] T. Damour and A. Nagar, Phys. Rev. D **76**, 064028 (2007), arXiv:0705.2519 [gr-qc].
[58] T. Damour, B. R. Iyer, and A. Nagar, Phys. Rev. D **79**, 064004 (2009), arXiv:0811.2069 [gr-qc].
[59] R. Fujita and B. R. Iyer, Phys. Rev. D **82**, 044051 (2010), arXiv:1005.2266 [gr-qc].
[60] Y. Pan, A. Buonanno, R. Fujita, E. Racine, and H. Tagoshi, Phys. Rev. D **83**, 064003 (2011), arXiv:1006.0431 [gr-qc].
[61] A. Buonanno, G. B. Cook, and F. Pretorius, Phys. Rev. D **75**, 124018 (2007), arXiv:gr-qc/0610122.
[62] A. Buonanno et al., Phys. Rev. D **76**, 104049 (2007), arXiv:0706.3732 [gr-qc].
[63] Y. Pan et al., Phys. Rev. D **77**, 024014 (2008), arXiv:0704.1964 [gr-qc].
[64] M. Boyle et al., Phys. Rev. D **78**, 104020 (2008), arXiv:0804.4184 [gr-qc].
[65] A. Buonanno et al., Phys. Rev. D **79**, 124028 (2009), arXiv:0902.0790 [gr-qc].
[66] Y. Pan et al., Phys. Rev. D **81**, 084041 (2010), arXiv:0912.3466 [gr-qc].
[67] T. Damour and A. Nagar, Phys. Rev. D **77**, 024043 (2008), arXiv:0711.2628 [gr-qc].
[68] T. Damour, A. Nagar, E. N. Dorband, D. Pollney, and L. Rezzolla, Phys. Rev. D **77**, 084017 (2008), arXiv:0712.3003 [gr-qc].
[69] T. Damour, A. Nagar, M. Hannam, S. Husa, and B. Brügmann, Phys. Rev. D **78**, 044039 (2008), arXiv:0803.3162 [gr-qc].
[70] T. Damour and A. Nagar, Phys. Rev. D **79**, 081503(R) (2009), arXiv:0902.0136 [gr-qc].
[71] Y. Pan et al., Phys. Rev. D **84**, 124052 (2011), arXiv:1106.1021 [gr-qc].
[72] A. Nagar, T. Damour, and A. Tartaglia, Class. Quant. Grav. **24**, S109 (2007), arXiv:gr-qc/0612096.
[73] S. Bernuzzi and A. Nagar, Phys. Rev. D **81**, 084056 (2010), arXiv:1003.0597 [gr-qc].
[74] S. Bernuzzi, A. Nagar, and A. Zenginoğlu, Phys. Rev. D **83**, 064010 (2011), arXiv:1012.2456 [gr-qc].
[75] S. Bernuzzi, A. Nagar, and A. Zenginoğlu, Phys. Rev. D **84**, 084026 (2011), arXiv:1107.5402 [gr-qc].
[76] N. Yunes, A. Buonanno, S. A. Hughes, M. Coleman Miller, and Y. Pan, Phys. Rev. Lett. **104**, 091102 (2010), arXiv:0909.4263 [gr-qc].
[77] N. Yunes et al., Phys. Rev. D **83**, 044044 (2011), arXiv:1009.6013 [gr-qc].
[78] E. Barausse et al., Phys. Rev. D **85**, 024046 (2012), arXiv:1110.3081 [gr-qc].
[79] T. Damour, Phys. Rev. D **81**, 024017 (2010), arXiv:0910.5533 [gr-qc].
[80] L. Barack and N. Sago, Phys. Rev. D **81**, 084021 (2010), arXiv:1002.2386 [gr-qc].
[81] L. Barack, T. Damour, and N. Sago, Phys. Rev. D **82**, 084036 (2010), arXiv:1008.0935 [gr-qc].
[82] N. Sago, L. Barack, and S. Detweiler, Phys. Rev. D **78**, 124024 (2008), arXiv:0810.2530 [gr-qc].
[83] A. G. Shah, T. S. Keidl, J. L. Friedman, D.-H. Kim, and L. R. Price, Phys. Rev. D **83**, 064018 (2011), arXiv:1009.4876 [gr-qc].
[84] L. Blanchet, S. Detweiler, A. Le Tiec, and B. F. Whiting, Phys. Rev. D **81**, 064004 (2010), arXiv:0910.0207 [gr-qc].
[85] L. Blanchet, S. Detweiler, A. Le Tiec, and B. F. Whiting, Phys. Rev. D **81**, 084033 (2010), arXiv:1002.0726 [gr-qc].
[86] L. Blanchet, S. Detweiler, A. Le Tiec, and B. F. Whiting, in *Mass and motion in general relativity*, edited by L. Blanchet, A. Spallicci, and B. Whiting (Springer, 2011), vol. 162 of *Fundamental Theories of Physics*, p. 415, arXiv:1007.2614 [gr-qc].
[87] A. Le Tiec, E. Barausse, and A. Buonanno (2011), arXiv:1111.5609 [gr-qc].
[88] A. Le Tiec, L. Blanchet, and B. F. Whiting (2011), arXiv:1111.5378 [gr-qc].
[89] A. Buonanno, Y. Chen, and M. Vallisneri, Phys. Rev. D **67**, 024016 (2003), *Erratum:* Phys. Rev. D **74**, 029903(E) (2006), arXiv:gr-qc/0205122.
[90] A. Le Tiec et al., Phys. Rev. Lett. **107**, 141101 (2011), arXiv:1106.3278 [gr-qc].
[91] T. Damour and A. Nagar, in *Mass and motion in general relativity*, edited by L. Blanchet, A. Spallicci, and B. Whiting (Springer, 2011), vol. 162 of *Fundamental Theories of Physics*, p. 211, arXiv:0906.1769 [gr-qc].
[92] L. Blanchet and T. Damour, Phil. Trans. Roy. Soc. Lond. A **320**, 379 (1986).
[93] L. Blanchet and T. Damour, Phys. Rev. D **37**, 1410 (1988).